

Original article

YC-1 induces G₀/G₁ phase arrest and mitochondria-dependent apoptosis in cisplatin-resistant human oral cancer CAR cells

Miau-Rong Lee¹, Chingju Lin², Chi-Cheng Lu^{3,6}, Sheng-Chu Kuo^{4,5}, Je-Wei Tsao³, Yu-Ning Juan³,
Hong-Yi Chiu⁶, Fang-Yu Lee⁷, Jai-Sing Yang^{3,*}, Fuu-Jen Tsai^{8,9,10,*}

¹Department of Biochemistry, China Medical University, Taichung 404, Taiwan

²Department of Physiology, China Medical University, Taichung 404, Taiwan

³Department of Medical Research, China Medical University Hospital, China Medical University, Taichung 404, Taiwan

⁴Chinese Medicinal Research and Development Center, China Medical University Hospital, China Medical University, Taichung 404, Taiwan

⁵School of Pharmacy, China Medical University, Taichung 404, Taiwan

⁶Department of Pharmacy, Buddhist Tzu Chi General Hospital, Hualien 970, Taiwan

⁷Yung-Shin Pharmaceutical Industry Co., Ltd., Tachia, Taichung 437, Taiwan

⁸Genetics Center, Department of Medical Research, China Medical University Hospital, Taichung 404, Taiwan

⁹School of Chinese Medicine, China Medical University, Taichung 404, Taiwan

¹⁰Department of Medical Genetics, China Medical University Hospital, Taichung 404, Taiwan

Received 10th of April 2017 Accepted 2nd of May 2017

© Author(s) 2017. This article is published with open access by China Medical University

Keywords:

YC-1;
G₀/G₁ phase arrest;
mitochondria;
Apoptosis;
CAR cells

ABSTRACT

Oral cancer is a serious and fatal disease. Cisplatin is the first line of chemotherapeutic agent for oral cancer therapy. However, the development of drug resistance and severe side effects cause tremendous problems clinically. In this study, we investigated the pharmacologic mechanisms of YC-1 on cisplatin-resistant human oral cancer cell line, CAR. Our results indicated that YC-1 induced a concentration-dependent and time-dependent decrease in viability of CAR cells analyzed by MTT assay. Real-time image analysis of CAR cells by IncuCyte™ Kinetic Live Cell Imaging System demonstrated that YC-1 inhibited cell proliferation and reduced cell confluence in a time-dependent manner. Results from flow cytometric analysis revealed that YC-1 promoted G₀/G₁ phase arrest and provoked apoptosis in CAR cells. The effects of cell cycle arrest by YC-1 were further supported by up-regulation of p21 and down-regulation of cyclin A, D, E and CDK2 protein levels. TUNEL staining showed that YC-1 caused DNA fragmentation, a late stage feature of apoptosis. In addition, YC-1 increased the activities of caspase-9 and caspase-3, disrupted the mitochondrial membrane potential ($\Delta\Psi_m$) and stimulated ROS production in CAR cells. The protein levels of cytochrome *c*, Bax and Bak were elevated while Bcl-2 protein expression was attenuated in YC-1-treated CAR cells. In summary, YC-1 suppressed the viability of cisplatin-resistant CAR cells through inhibiting cell proliferation, arresting cell cycle at G₀/G₁ phase and triggering mitochondria-mediated apoptosis. Our results provide evidences to support the potentially therapeutic application of YC-1 on fighting against drug resistant oral cancer in the future.

1. Introduction

According to the 2014 annual report of the Ministry of Health and Welfare, R.O.C. (Taiwan), cancer is the first leading cause of death among the ten leading chronic diseases in Taiwan. The number of cancer death reports was 46,829 (28,776 in men and 18,053 in women), accounting for 28.6% of the total number

of deaths. The death rate was 199.6 per 100,000 population, increased by 1.3% from 2013 to 2014 [1, 2]. Oral cancer is the fifth leading cause of cancer death in Taiwan. The death rate of oral cancer was 11.4 per 100,000 population [1, 2]. In Taiwan, the major risk factors of oral cancer are betel nut chewing [3-6], smoking [7], alcohol consumption [4, 8], inflammation [9, 10] and human papilloma virus (HPV) infection [11, 12]. The 5-year

*Corresponding author. Department of Medical Research, China Medical University Hospital, China Medical University, No. 2, Yuh-Der Road, Taichung 40447, Taiwan.

E-mail addresses: jaisingyang@gmail.com (J.-S. Yang), d0704@mail.cmuh.org.tw (F.-J. Tsai).

survival rate of oral cancer is 50% [13, 14]. Surgery, radiotherapy and chemotherapeutic drugs are the major treatments for oral cancer. The first-line chemotherapeutic drugs to treat oral cancer are cisplatin, carboplatin, 5-fluorouracil (5-FU), paclitaxel (Taxol®) and docetaxel (Taxotere®) [15-17]. However, surgery, radiotherapy and chemotherapy did not significantly improve the overall survival rate of oral cancer patients. On top of that, the development of drug resistance in the duration of chemotherapy remains as a clinical obstacle [18, 19]. To meet the need, designing novel compounds as well as discovering new targeting molecules that can overcome the resistance to chemotherapeutic drugs in oral cancer are clinically important.

YC-1 [3-(5'-hydroxymethyl-2'-furyl)-1-benzylindazole] was first designed and synthesized in our team [20, 21]. Current studies have shown that YC-1 has a wide spectrum of pharmacological activities, including anti-platelet [22-24], anti-inflammatory [25-29], anti-angiogenesis [30], neuro-protective [31-33], anti-hepatic fibrosis [34] and anti-cancer properties [20, 33, 35-56]. The underlying mechanism exerted by YC-1 included activation of NO-independent soluble guanylyl cyclase (sGC), inactivation of phosphodiesterase type 5 (PDE5) [29, 57, 58] and inhibition of hypoxia-inducible factor 1 α (HIF-1 α) activity [22, 59, 60]. As for the anti-cancer activity, YC-1 can repress the proliferation of various types of cancer cells, including head and neck squamous cell carcinoma [48], esophageal squamous carcinoma [43], lung cancer [61-65], lymphoma [66, 67], bladder cancer [41, 68], hepatocellular carcinoma [52, 69], breast cancer [35, 55, 70], neuroblastoma [32], ovarian carcinoma [71], prostate cancer [72], pancreatic cancer [73], renal carcinoma [56, 74, 75], osteosarcoma [45], colon cancer [76, 77] and leukemia [20, 39, 49, 78]. In terms of the molecular mechanisms in anti-cancer activity, YC-1 induced cell cycle arrest at G₀/G₁ phase [50, 79, 80] or at S phase [52, 81], inhibited multidrug-resistant protein (MDR1) [82], reduced autophagy [83] and triggered apoptotic cell death [52]. In addition, YC-1 enhanced chemotherapeutic cisplatin sensitivity in hepatocellular carcinoma cells [84] and head and neck squamous cell carcinoma cells [48]. However, studies on whether YC-1 can inhibit cisplatin-resistant human oral cancer are scarce. The objective of this study was to investigate the anti-cancer effects of YC-1 on cisplatin-resistant human tongue squamous cell carcinoma CAR cells and its underlying mechanisms.

2. Material and methods

2.1. Chemicals and reagents

Cisplatin, propidium iodide (PI) and thiazolyl blue tetrazolium bromide (MTT) were purchased from Sigma-Aldrich (St. Louis, MO, USA). Trypsin-EDTA was purchased from BioConcept (Allschwil/BL, Switzerland). Fetal bovine serum (FBS), L-glutamine, penicillin G, 2',7'-dichlorodihydrofluorescein diacetate (H₂DCFDA) and 3,3-dihexyloxa-carbocyanine iodide [DiOC₆(3)] were obtained from Thermo Fisher Scientific (Carlsbad, CA, USA). Caspase-3 and caspase-9 activity assay kits were purchased from R&D Systems Inc. (Minneapolis, MN, USA). The primary antibodies against Bcl-2, Bax, cytochrome *c*, Apaf-1, AIF, p21, cyclin A, cyclin D, cyclin E, CDK 2, β -actin and the goat anti-rabbit or anti-mouse IgG-horseradish peroxidase (HRP) secondary antibodies were purchased from GeneTex, (Hsinchu, Taiwan). Pan-caspase inhibitor (z-VAD-fmk) and enhanced chemiluminescence (ECL) detection kit (Immobilon Western

Chemiluminescent HRP Substrate) were purchased from Merck Millipore (Billerica, MA, USA). YC-1 was designed and synthesized as detailed in the previous study [21].

2.2. Cell culture

The cisplatin-resistant cell line (CAR) was developed by treating CAL 27 cell line, a parental human tongue squamous cell carcinoma (American Type Culture Collection, Manassas, VA, USA) with 10-80 μ M of cisplatin. CAR cells are characterized by its stable resistance to cisplatin as previously described [1, 18, 85, 86]. The cells were cultured in Dulbecco's modified Eagle's medium (DMEM) fortified with 10% fetal bovine serum (FBS), 100 U/ml penicillin, 100 μ g/ml streptomycin, and 2 mM L-glutamine (Thermo Fisher Scientific) and were incubated at 37°C with a humidified 5% CO₂ air. The cisplatin-resistant CAR cells were constantly cultured in medium containing 80 μ M cisplatin unless otherwise indicated [1, 18, 85, 86].

2.3. Cell viability assay

CAR cells (1×10^4 cells/per well) were seeded in 96-well plates in 100 μ l medium with or without 25, 50, 75 and 100 μ M of YC-1 for 24 h. After YC-1 treatment, DMEM containing 500 μ g/ml of MTT was added and incubated at 37°C for 4 h. The medium was then removed, and 100 μ l DMSO was added to each well to dissolve the formed blue formazan crystals, followed by measuring the 570 nm absorbance of each well by the ELISA plate reader with a reference wavelength of 620 nm. For the caspase inhibition experiment, cells were pretreated with 15 μ M z-VAD-fmk (a pan-caspase inhibitor) for 1 h before subjected to YC-1 administration. Cell morphological examination was observed and photographed by the IncuCyte™ Kinetic Live Cell Imaging System (Essen BioScience, Ann Arbor, MI, USA) [87-89].

2.4. IncuCyte cell proliferation and confluence assay

To measure the cell confluence, a stable mixture of CAR cells (2×10^4 cells) were plated into a 96-well plate. The cells were then incubated with or without 25, 50, 75 and 100 μ M of YC-1. Cell confluence relative to the control cells was determined by the IncuCyte™ Kinetic Live Cell Imaging System (Essen BioScience) at a 2-h interval and up to 48 h [90].

2.5. Flow cytometry analysis of cell cycle distribution

CAR cells (2×10^5 cells/per well) were plated into the 12-well plates and then treated with 100 μ M of YC-1 for 0, 12, 24, 36 and 48 h. The cells were then fixed, followed by staining with propidium iodide (PI) solution as previously described [91, 92]. The cell cycle profiling and the data analysis were determined utilizing a Muse Cell Analyzer (Merck Millipore, Hayward, CA, USA) [93-98].

2.6. Immunoblotting analysis

CAR cells (1×10^7 /75-T flask) were treated with 0, 25, 50, 75 and 100 μ M of YC-1 for 48 h. The cells were then harvested, and the total proteins in cell lysate were collected by SDS sample buffer. Briefly, protein sample from each treatment was subjected to electrophoresis on a 10% SDS-polyacrylamide gel (SDS-PAGE), followed by electro-transferring to a PVDF membrane.

The transferred membranes were blocked in 20 mM Tris-buffered saline/0.05% Tween-20 solution containing 5% non-fat dry milk for 1 h at room temperature. The membrane was then probed with the primary antibodies against proteins associated with either cell cycle regulation or apoptosis at 4°C overnight. Afterwards, the membranes were washed with Tris-buffered saline/Tween-20 and incubated with secondary antibodies conjugated with horseradish peroxidase (HRP). The blots were developed by an enhanced chemiluminescence kit (Immobilon Western HRP Substrate; Merck Millipore, Bedford, MA, USA), followed by X-ray film exposure [99, 100].

2.7. TUNEL staining

CAR cells (2×10^5 cells/ per well) were seeded into 12-well plates and incubated with 0, 25, 50, 75 and 100 μM of YC-1 for 48 h. At the end of the treatment, apoptotic DNA fragmentation was detected using the *In Situ* Cell Death Detection kit, Fluorescein (Roche Diagnostics GmbH, Roche Applied Science, Mannheim, Germany) according to the protocol by the manufacturer [101-104].

2.8. Assays for caspase-3 and caspase-9 activities

CAR cells (2×10^5 cells/ per well) were seeded into 6-well plates and incubated with 0, 25, 50, 75 and 100 μM of YC-1 for 48 h. At the end of the treatment, cells were harvested and cell lysates were assessed in accordance with the manufacturer's instruction provided in the caspase-3 and caspase-9 Colorimetric Assay kits (R&D Systems Inc.). Cell lysate protein was then incubated for 1 h at 37°C with specific caspase-3 substrate (DEVD-pNA) or caspase-9 substrate (LEHD-pNA) in the reaction buffer (provided in the kits). The OD₄₀₅ of the released pNA in each sample was measured as previously described [86, 105].

2.9. Detection of ROS generation and mitochondrial membrane potential ($\Delta\Psi\text{m}$)

CAR cells (2×10^5 cells/ per well) were seeded into 6-well plates and incubated with 0, 25, 50, 75 and 100 μM of YC-1 for 48 h. At the end of the treatment, cells were harvested and incubated with 10 μM H₂DCFDA and 4 nM DiOC₆ at 37°C for 30 min for H₂O₂ detection and $\Delta\Psi\text{m}$, respectively. The mean fluorescence intensity (MFI) was quantified by BD CellQuest Pro software (BD Biosciences, San Jose, CA, USA) after analysis by flow cytometry [86, 105, 106].

2.10. Statistical analysis

All the statistical results are presented as the mean \pm SD for at least three separate experiments. Statistical analysis of data was done using one-way ANOVA followed by Student's *t*-test. ****P*<0.001 was considered statistically significant.

3. Results

3.1. YC-1 decreased the viability and suppressed confluence of CAR cells

The cisplatin-resistant human oral CAR cells were treated with YC-1 (0, 25, 50 and 100 μM) for either 24 h or 48 h. The MTT

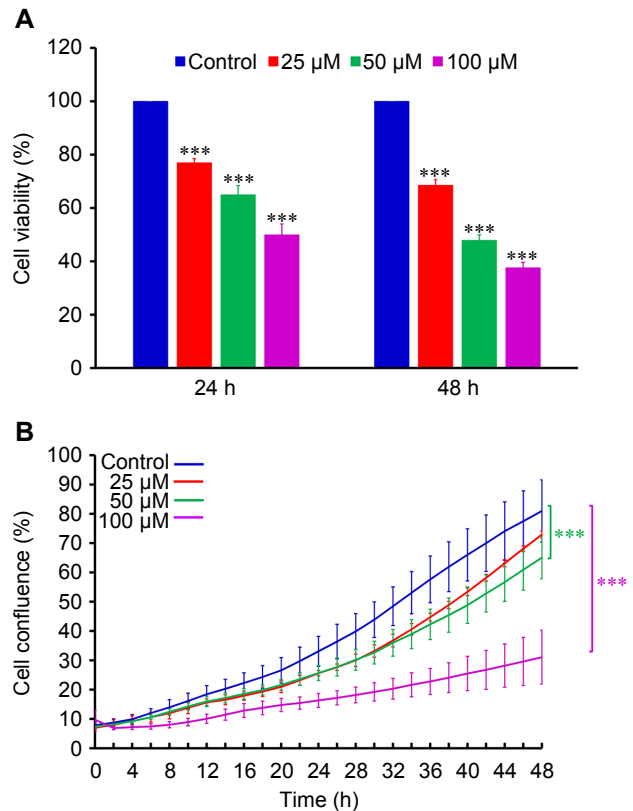


Fig. 1 - Effects of YC-1 on cell viability and cell confluence in CAR cells. Cells were incubated with 0, 25, 50 and 100 μM of YC-1 for various duration. (A) The cell viability was determined by MTT assay. (B) The cell confluence was determined by the IncuCyte™ Kinetic Live Cell Imaging System. Data are presented as the mean \pm SD (n = 3). **p*<0.001 versus untreated control.**

assay demonstrated that YC-1 significantly decreased the cell viability in a concentration and time-dependent manner (Fig. 1A). The percentage of cell confluence relative to the control cells was determined by the IncuCyte™ Kinetic Live Cell Imaging System at a 2-h interval and up to 48 h. The administration of YC-1 (0, 25, 50 and 100 μM) inhibited the confluences of cultured CAR cells (Fig. 1B). The inhibition of cell confluence showed concentration and time-dependent. Images of cultured CAR cells under different YC-1 concentrations (0, 25, 50 and 100 μM) taken by IncuCyte™ Kinetic Live Cell Imaging System at the indicated period of time showed that YC-1 induced cell morphology changes and triggered cell death (Fig. 2). Herein, we also provide the real-time cell imaging of cultured CAR cells with or without YC-1 (100 μM) by IncuCyte™ Kinetic Live Cell Imaging System video (Supplementary video). Our data revealed that YC-1 exhibited cytotoxicity to CAR cells.

3.2. YC-1 caused G₀/G₁ cell cycle arrest and affected the expression levels of G₀/G₁ proteins of CAR cells

To verify whether YC-1 treatment affects the cell cycle distribution, CAR cells were administered with 100 μM of YC-1 for 0, 12, 24, 36 and 48 h. The percentage of cells in G₀/G₁, S and G₂/M phase were analyzed by DNA content stained with PI and flow cytometry. Our data indicated that YC-1 treatment resulted in

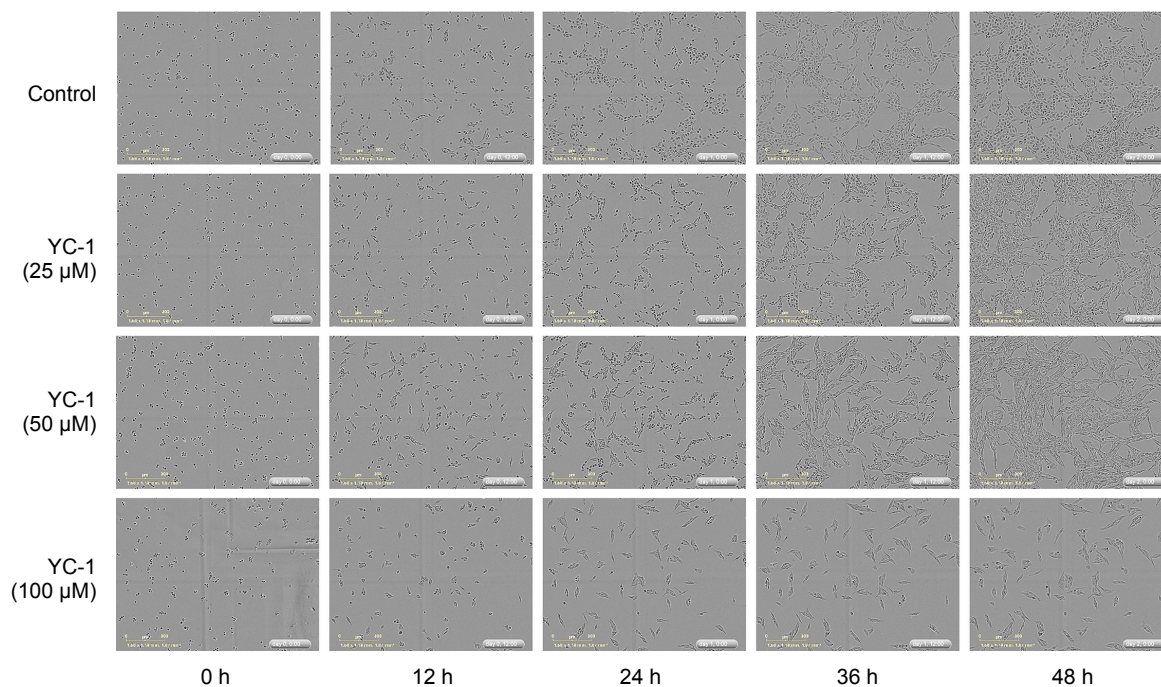


Fig. 2 - Effects of YC-1 on cell morphology and confluence of CAR cells. Cells were incubated with 0, 25, 50 and 100 μM of YC-1 for 0, 12, 24, 36 and 48 h. The cell morphology and density was determined by the IncuCyte™ Kinetic Live Cell Imaging System.

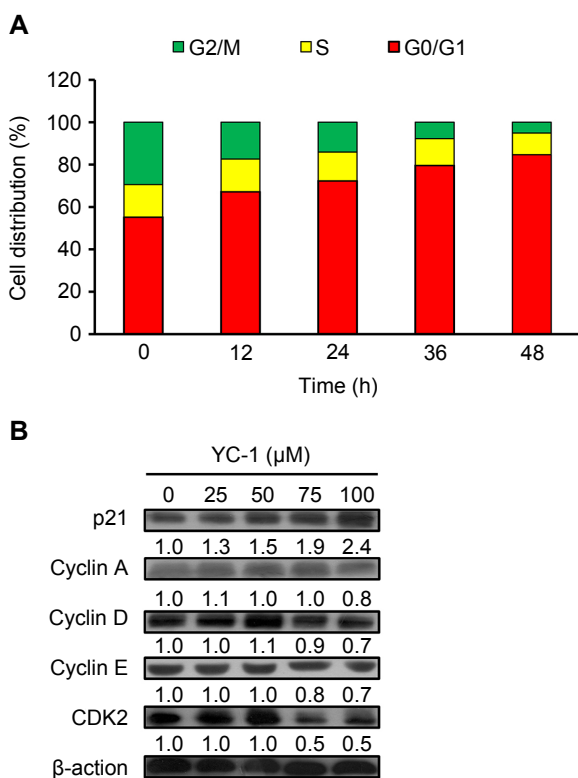


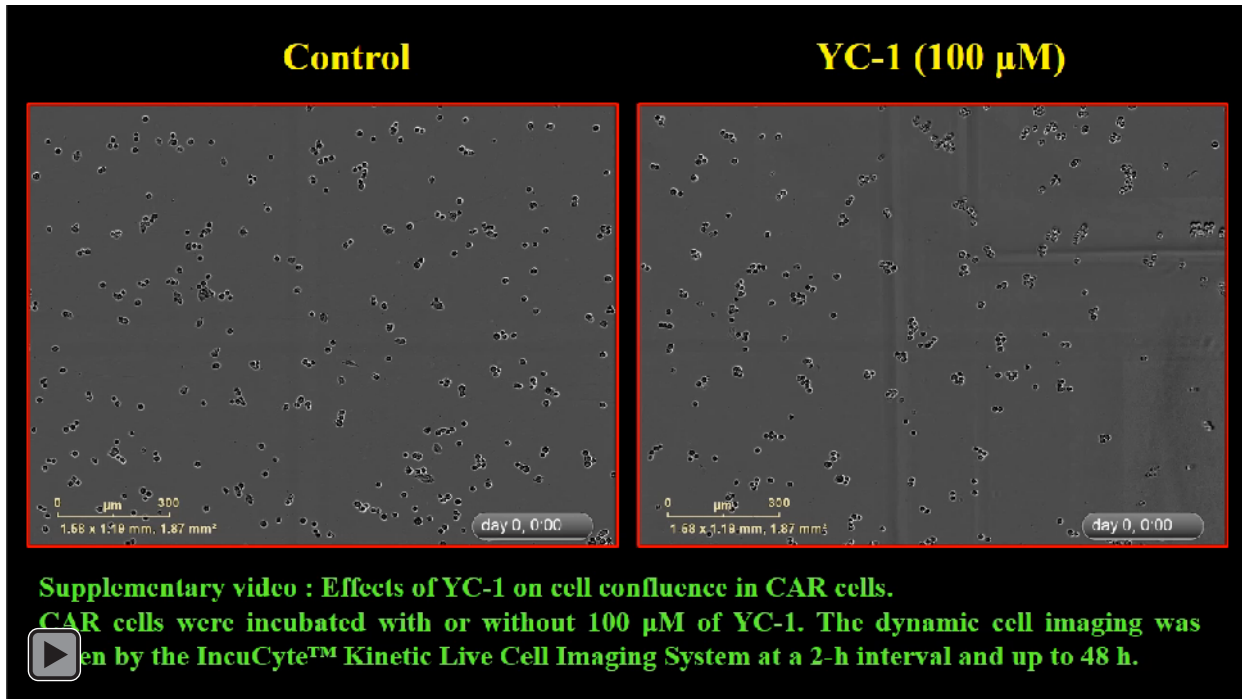
Fig. 3 - Effects of YC-1 on cell cycle distribution and the levels of G_0/G_1 proteins of CAR cells. (A) Cells were incubated with 100 μM of YC-1 for 0, 12, 24, 36 and 48 h. The cell cycle distribution was assessed by PI staining and flow cytometric analysis. (B) Whole-cell lysates were prepared, and the levels of G_0/G_1 proteins were analyzed by western blot analysis.

cell cycle arrest at G_0/G_1 phase. The percentage of cells arrested at G_0/G_1 increased as the treatment duration lengthened. In the meanwhile, a marked decrease of the cells at G_2/M phase was observed (Fig. 3A). The expression levels of proteins associated with G_0/G_1 were analyzed after 24-h treatment. YC-1 induced the protein expression of p21 in a concentration-dependent manner, while the protein expression of cyclins A, D, E and CDK2 was inhibited (Fig. 3B). These results indicated that YC-1 regulated CDK2 activation and caused G_0/G_1 phase arrest in the CAR cells.

3.3. YC-1 induced DNA fragmentation and enhanced caspase-9 and caspase-3 activities in CAR cells.

We examined whether YC-1 induces apoptosis in CAR cells. A significant reduction in cell viability from MTT assay was observed after cells were exposed to 100 μM of YC-1 for 48 h. However, the decreased cell viability induced by YC-1 was reversed by z-VAD-fmk (a pan-caspase inhibitor) (Fig. 4A). Results from TUNEL staining also showed that as the YC-1 concentration increased, more TUNEL positive cells were observed, indicating that more cells exhibited DNA fragmentation (Fig. 4B). To further investigate whether the cell death provoked by YC-1 was mediated through caspases activation, protein samples collected from CAR cells after YC-1 exposure for 48 h were analyzed. Treatment of YC-1 (0, 25, 50, 75 and 100 μM) significantly and concentration-dependently stimulated the activities of both caspases-9 and caspase-3 (Fig. 4C and 4D). Our data demonstrated that YC-1 induced apoptosis, and the activation of caspases was involved in apoptotic cell death in CAR cells.

3.4. YC-1 stimulated ROS production, collapsed mitochondrial membrane potential ($\Delta\Psi_m$) and altered the levels of apoptosis-related proteins in CAR cells



Supplementary video - Effects of YC-1 on cell confluence in CAR cells. Cells were incubated with or without 100 μM of YC-1. The dynamic cell imaging was taken by the IncuCyte™ Kinetic Live Cell Imaging System at a 2-h interval and up to 48 h.

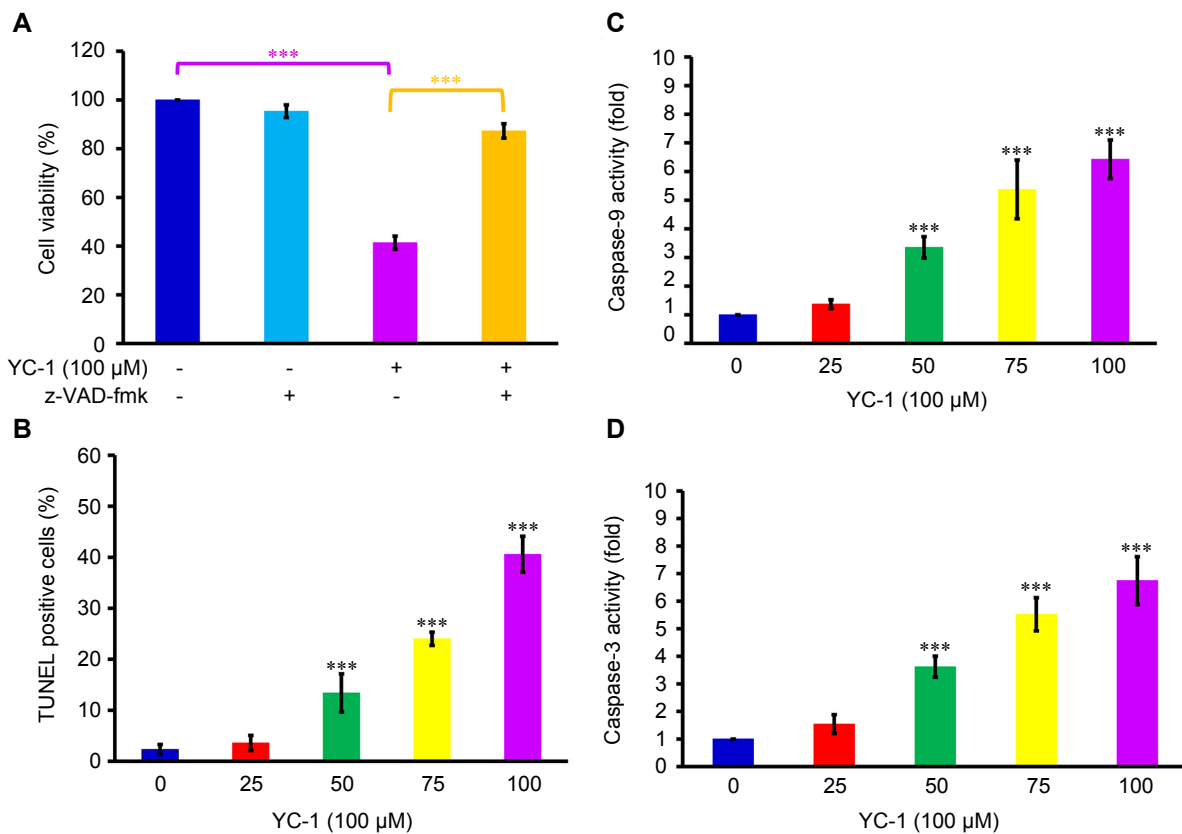


Fig. 4 - Effects of YC-1 on DNA fragmentation, caspase-9 and caspase-3 activities in CAR cells. (A) Cells were incubated with 100 μM of YC-1 with or without z-VAD-fmk for 48 h. The cell viability was determined by MTT assay. (B) TUNEL assay, (C) caspase-9 and (D) caspase-3 activities were analyzed in CAR cells treated with 0, 25, 50, 75 and 100 μM of YC-1 for 48 h. Data are presented as the mean \pm SD (n = 3). *** P <0.001 versus untreated control.

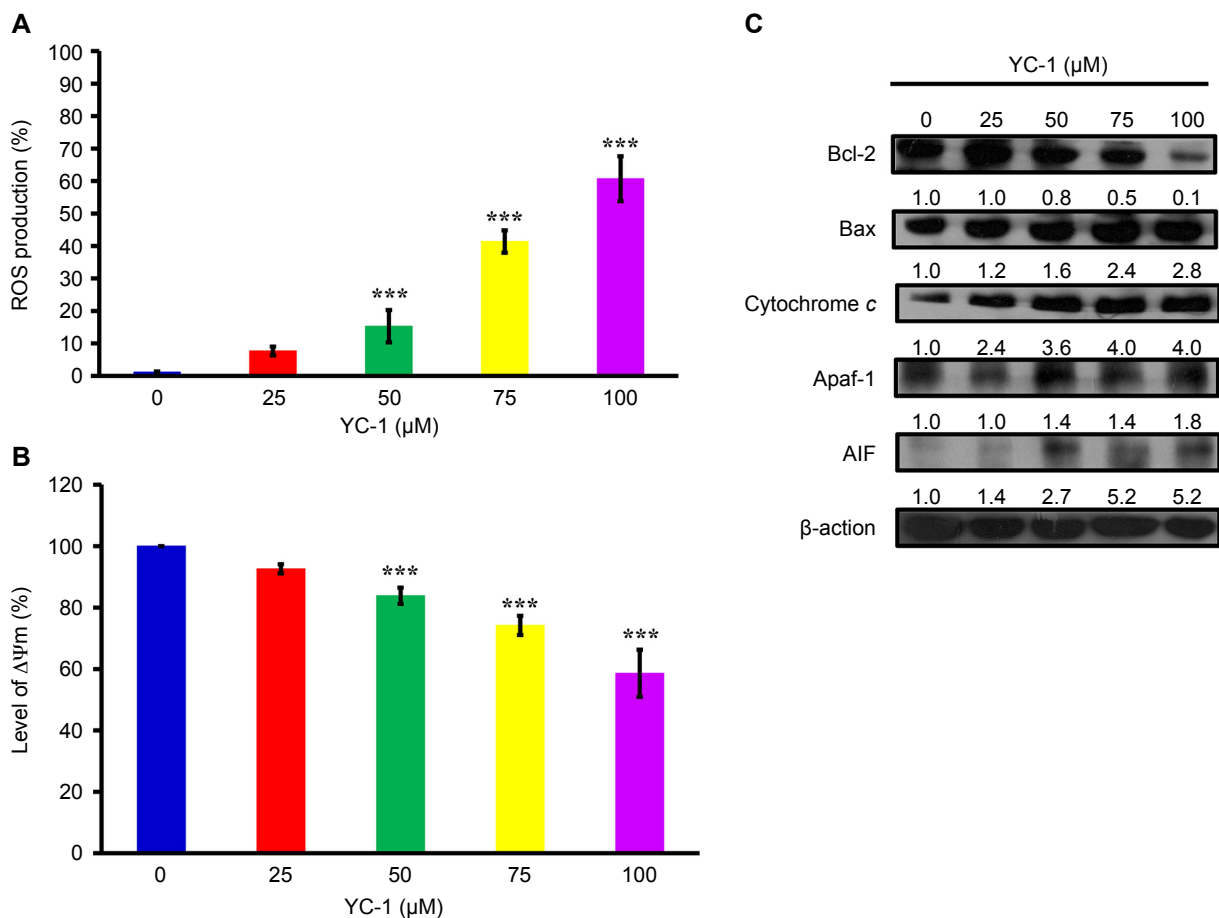


Fig. 5 - Effects of YC-1 on ROS, mitochondrial membrane potential ($\Delta\Psi_m$) and the levels of apoptosis-related proteins in CAR cells. Cells were incubated with 0, 25, 50, 75 and 100 μM of YC-1 for 48 h. (A) ROS level was assessed by staining with H_2DCFDA , and (B) loss of $\Delta\Psi_m$ was measured with $\text{DiOC}_6(3)$ by flow cytometry. Data are presented as the mean \pm SD (n=3). *** $P < 0.001$ versus untreated control. (C) Whole-cell lysates were prepared, and the levels of apoptosis related proteins were analyzed by western blot analysis. Data is presented.

We investigated whether YC-1 stimulates ROS production. The production of ROS markedly elevated after cells were administered with of YC-1 (0, 25, 50, 75 and 100 μM), and the elevation showed concentration-dependent (Fig. 5A). To confirm whether the mitochondrial pathway mediating YC-1-induced cell apoptosis, the level of $\Delta\Psi_m$ was measured, and immunoblotting analysis was performed to evaluate the expression levels of proteins associated with mitochondria-dependent apoptotic pathways. CAR cells exhibited a decrease of $\Delta\Psi_m$ in a concentration-dependent manner after 48 h of YC-1 treatment (Fig. 5B). YC-1 suppressed the level of Bcl-2, while it promoted the protein expressions of Bax, cytochrome *c*, Apaf-1 and AIF (Fig. 5C), indicating the involvement of mitochondria-dependent pathway.

4. Discussion

Discovering and exploring novel therapeutic strategy and underlying molecular mechanisms has been a major research focus in oral cancer therapy [107-110]. Studies on various cancer cells demonstrated that YC-1 possessed significant anti-cancer activities through several pathways. YC-1 can induce cell cycle arrest [81, 111, 112], apoptosis [81, 111, 112] and autophagy [83, 113,

114]. It also blocked angiogenesis [30, 115-117], cell migration [41, 43, 72, 118], metastasis [36, 64, 119] and reduce matrix metalloproteinases (MMPs) activity [41, 72, 117]. Furthermore, YC-1 enhanced the chemo-sensitivity of cancer cells to cisplatin by regulating expression and activity of apoptosis-related proteins, leading to the activation of caspase-9 and caspase-3 signaling [120]. Recently, Tuttle *et al.* [48] reported that YC-1 inhibited cell proliferation, induced apoptotic cell death, and increased sensitivity to cisplatin in UM-1- and CAL 27-cisplatin resistance cells. However, the molecular mechanisms of YC-1-induced cell cycle arrest and death in cisplatin resistant oral cancer cells are not yet fully understood. In this study, our results showed that 25-100 μM of YC-1 significantly inhibited the proliferation of cisplatin-resistant CAR cells (Fig. 1, Fig. 2 and Supplementary video). YC-1 treatment increased the number of cells in the G_0/G_1 phase, suggesting that YC-1 caused growth inhibition by promoting G_0/G_1 phase arrest in CAR cells (Fig. 3). The significant DNA fragmentation and caspase-3/-9 activation in YC-1 treated cells (Fig. 4B, C, and D) indicate that YC-1 can induce caspase-dependent apoptosis in CAR cells. Our findings provide new insights addressing the anti-cancer activity of YC-1 in cisplatin-resistant CAR cells at the molecular levels.

Once the mitochondrial apoptotic signaling is provoked,

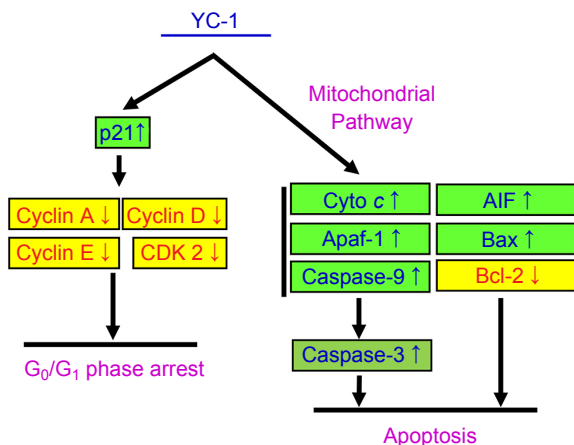


Fig. 6 - Schematic diagram of proposed molecular mechanism of YC-1-induced G₀/G₁ phase arrest and apoptosis in cisplatin-resistant human oral cancer CAR cells.

changes in the mitochondrial membrane permeability would lead to the loss of mitochondrial membrane potential. In addition, the mitochondrial outer membrane becomes leaky and releases the pro-apoptotic proteins; including cytochrome *c*, Apaf-1, procaspase-9, AIF and Endo G into cytosol. These proteins can then activate caspase-9 and caspase-3 and result in DNA fragmentation, a unique feature of the late stage apoptosis [121-125]. Bcl-2 family proteins are also involved in the regulation of apoptosis through modulating mitochondrial functions [121, 124]. Our results showed that YC-1 induced apoptosis, as evidenced by the reduced viability and the significant number of TUNEL-positive cells (Fig 4A, B). YC-1 induced apoptosis was further confirmed by pan-caspase inhibitor which reversed the reduction of cellular viability in YC-1 treated cells (Fig 4A). In addition, the loss of $\Delta\Psi_m$, elevation of ROS production, and the changes in quantity of mitochondria-related proteins (Bcl-2, Bax, cytochrome *c*, Apaf-1 and AIF) were observed after YC-1 treatment (Fig. 5). These results suggested that YC-1-induced apoptosis was mediated through the activation of caspase cascades, and this apoptotic death was mitochondria-dependent. This study is the first report to prove the involvement of a mitochondrial pathway in YC-1-induced apoptosis in cisplatin-resistant CAR cells.

It has been documented that YC-1 inhibited cell proliferation and cell cycle progression from G₀/G₁ to S phase in rat mesangial cell and human hepatocellular carcinoma cells [50, 80]. Teng *et al.* [50] demonstrated that YC-1 inhibited human hepatocellular carcinoma cell proliferation through G₀/G₁ phase arrest and increased p21 and p27 protein levels. However, Yeo. *et al.* reported YC-1 induced S phase arrest and apoptosis in Hep3B cells [81]. Our results (Fig 3) were consistent with those of Teng *et al.* [50] and suggested that, by down-regulation of CDK2/cyclin A,D, and E activities, YC-1 blocked cell cycle at G₀/G₁ phase.

The IncuCyte™ Kinetic Live Cell Imaging System provides a continuous time-lapsed recording and quantitation of cell life images, which facilitates a robust data collection and analysis. This system can be used to detect cell activities such as cell proliferation, migration, invasion, wound healing, caspase activity and autophagy [126-128]. In the present study, we are the first group using this imaging system to characterize cell proliferation and confluence in YC-1-treated CAR cells (Fig. 2 and Supplementary video). Thus, more studies on anti-cancer activity of YC-1 can

be accelerated and examined by this cell image system in the near future.

5. Conclusions

Fig. 6 illustrated the proposed molecular mechanism of YC-1-provoked G₀/G₁ phase arrest and apoptosis in CAR cells. Our results revealed that YC-1 arrested at G₀/G₁ phase through regulating p21, cyclin A, D, E and CDK2 activity. In addition, YC-1 induced apoptosis in CAR cells *via* caspases activation and mitochondria-dependent pathway. YC-1 is proved to be potential adjuvants or alternatives to cisplatin treatment in cisplatin-resistant oral cancer.

Competing interests

The authors declare that they have no competing interests.

Acknowledgments

This work was supported by the grant from China Medical University Hospital, Taichung, Taiwan (DMR-106-122). The authors also would like to express our gratitude to Mr. Meng-Jou Liao (Tekon Scientific Corp.), Mr. Chin-Chen Lin (Tekon Scientific Corp.) and Mr. Chang-Wei Li (AllBio Science Incorporated, Taiwan) for their excellent technique and equipment supports.

Open Access This article is distributed under terms of the Creative Commons Attribution License which permits any use, distribution, and reproduction in any medium, provided original author(s) and source are credited.

REFERENCES

- [1] Yuan CH, Horng CT, Lee CF, Chiang NN, Tsai FJ, Lu CC, *et al.* Epigallocatechin gallate sensitizes cisplatin-resistant oral cancer CAR cell apoptosis and autophagy through stimulating AKT/STAT3 pathway and suppressing multidrug resistance 1 signaling. *Environ Toxicol.* 2017; 32: 845-55.
- [2] Chuang SL, Su WW, Chen SL, Yen AM, Wang CP, Fann JC, *et al.* Population-based screening program for reducing oral cancer mortality in 2,334,299 Taiwanese cigarette smokers and/or betel quid chewers. *Cancer.* 2017; 123: 1597-609.
- [3] Tsai KY, Su CC, Chiang CT, Tseng YT, Lian IB. Environmental heavy metal as a potential risk factor for the progression of oral potentially malignant disorders in central Taiwan. *Cancer Epidemiol.* 2017; 47: 118-24.
- [4] Chou CH, Chou YE, Chuang CY, Yang SF, Lin CW. Combined effect of genetic polymorphisms of AURKA and environmental factors on oral cancer development in Taiwan. *PLoS One.* 2017; 12: e0171583.
- [5] Chan CY, Lien CH, Lee MF, Huang CY. Quercetin suppresses cellular migration and invasion in human head and neck squamous cell carcinoma (HNSCC). *Biomedicine (Taipei).* 2016; 6: 15.
- [6] Huang YP, Chang NW. PPARalpha modulates gene expression

- profiles of mitochondrial energy metabolism in oral tumorigenesis. *Biomedicine (Taipei)*. 2016; 6: 3.
- [7] Butler C, Lee YA, Li S, Li Q, Chen CJ, Hsu WL, *et al.* Diet and the risk of head-and-neck cancer among never-smokers and smokers in a Chinese population. *Cancer Epidemiol*. 2017; 46: 20-26.
- [8] Wang WH, Hsuan KY, Chu LY, Lee CY, Tyan YC, Chen ZS, *et al.* Anticancer Effects of *Salvia miltiorrhiza* Alcohol Extract on Oral Squamous Carcinoma Cells. *Evid Based Complement Alternat Med*. 2017; 2017: 5364010.
- [9] Lien MY, Lin CW, Tsai HC, Chen YT, Tsai MH, Hua CH, *et al.* Impact of CCL4 gene polymorphisms and environmental factors on oral cancer development and clinical characteristics. *Oncotarget* 2017.
- [10] Tien AJ, Chien CY, Chen YH, Lin LC, Chien CT. Fruiting Bodies of *Antrodia cinnamomea* and Its Active Triterpenoid, Antcin K, Ameliorates N-Nitrosodiethylamine-Induced Hepatic Inflammation, Fibrosis and Carcinogenesis in Rats. *Am J Chin Med*. 2017; 45: 173-98.
- [11] Ragin C, Liu JC, Jones G, Shoyele O, Sowunmi B, Kennett R, *et al.* Prevalence of HPV Infection in Racial-Ethnic Subgroups of Head and Neck Cancer Patients. *Carcinogenesis*. 2016.
- [12] Huang SF, Li HF, Liao CT, Wang HM, Chen IH, Chang JT, *et al.* Association of HPV infections with second primary tumors in early-staged oral cavity cancer. *Oral Dis*. 2012; 18: 809-15.
- [13] Suzuki R, Matsushima Y, Okudaira N, Sakagami H, Shirataki Y. Cytotoxic Components Against Human Oral Squamous Cell Carcinoma Isolated from *Andrographis paniculata*. *Anticancer Res*. 2016; 36: 5931-35.
- [14] Kumar M, Nanavati R, Modi TG, Dobariya C. Oral cancer: Etiology and risk factors: A review. *J Cancer Res Ther*. 2016; 12: 458-63.
- [15] Schmaltz H, Borel C, Ciftci S, Takeda-Raguin C, Debry C, Schultz P, *et al.* Induction chemotherapy before surgery for unresectable head and neck cancer. *B-ENT*. 2016; 12: 29-32.
- [16] Noronha V, Patil V, Joshi A, Muddu V, Bhattacharjee A, Juvekar S, *et al.* Is taxane/platinum/5 fluorouracil superior to taxane/platinum alone and does docetaxel trump paclitaxel in induction therapy for locally advanced oral cavity cancers? *Indian J Cancer*. 2015; 52: 70-3.
- [17] Chung CH, Rudek MA, Kang H, Marur S, John P, Tsottles N, *et al.* A phase I study afatinib/carboplatin/paclitaxel induction chemotherapy followed by standard chemoradiation in HPV-negative or high-risk HPV-positive locally advanced stage III/IVa/IVb head and neck squamous cell carcinoma. *Oral Oncol*. 2016; 53: 54-9.
- [18] Chang CH, Lee CY, Lu CC, Tsai FJ, Hsu YM, Tsao JW, *et al.* Resveratrol-induced autophagy and apoptosis in cisplatin-resistant human oral cancer CAR cells: A key role of AMPK and Akt/mTOR signaling. *Int J Oncol*. 2017; 50: 873-82.
- [19] Ding L, Ren J, Zhang D, Li Y, Huang X, Ji J, *et al.* The TLR3 Agonist Inhibit Drug efflux and Sequentially Consolidates Low-dose Cisplatin-based Chemoimmunotherapy while Reducing Side effects. *Mol Cancer Ther*. 2017.
- [20] Chung JG, Yang JS, Huang LJ, Lee FY, Teng CM, Tsai SC, *et al.* Proteomic approach to studying the cytotoxicity of YC-1 on U937 leukemia cells and antileukemia activity in orthotopic model of leukemia mice. *Proteomics*. 2007; 7: 3305-17.
- [21] Lee FY, Lien JC, Huang LJ, Huang TM, Tsai SC, Teng CM, *et al.* Synthesis of 1-benzyl-3-(5'-hydroxymethyl-2'-furyl)indazole analogues as novel antiplatelet agents. *J Med Chem*. 2001; 44: 3746-9.
- [22] Chun YS, Yeo EJ, Park JW. Versatile pharmacological actions of YC-1: anti-platelet to anticancer. *Cancer Lett*. 2004; 207: 1-7.
- [23] Nakane M. Soluble guanylyl cyclase: physiological role as an NO receptor and the potential molecular target for therapeutic application. *Clin Chem Lab Med*. 2003; 41: 865-70.
- [24] Tulis DA, Bohl Masters KS, Lipke EA, Schiesser RL, Evans AJ, Peyton KJ, *et al.* YC-1-mediated vascular protection through inhibition of smooth muscle cell proliferation and platelet function. *Biochem Biophys Res Commun*. 2002; 291: 1014-21.
- [25] Yun S, Lee SH, Kang YH, Jeong M, Kim MJ, Kim MS, *et al.* YC-1 enhances natural killer cell differentiation from hematopoietic stem cells. *Int Immunopharmacol*. 2010; 10: 481-6.
- [26] Lu DY, Tang CH, Liou HC, Teng CM, Jeng KC, Kuo SC, *et al.* YC-1 attenuates LPS-induced proinflammatory responses and activation of nuclear factor-kappaB in microglia. *Br J Pharmacol*. 2007; 151: 396-405.
- [27] Hwang TL, Hung HW, Kao SH, Teng CM, Wu CC, Cheng SJ. Soluble guanylyl cyclase activator YC-1 inhibits human neutrophil functions through a cGMP-independent but cAMP-dependent pathway. *Mol Pharmacol*. 2003; 64: 1419-27.
- [28] Wu SN. Large-conductance Ca²⁺-activated K⁺ channels: physiological role and pharmacology. *Curr Med Chem*. 2003; 10: 649-61.
- [29] Ko FN, Wu CC, Kuo SC, Lee FY, Teng CM. YC-1, a novel activator of platelet guanylate cyclase. *Blood*. 1994; 84: 4226-33.
- [30] Wang J, Li G, Wang Y, Tang S, Sun X, Feng X, *et al.* Suppression of tumor angiogenesis by metformin treatment *via* a mechanism linked to targeting of HER2/HIF-1alpha/VEGF secretion axis. *Oncotarget*. 2015; 6: 44579-92.
- [31] Na JI, Na JY, Choi WY, Lee MC, Park MS, Choi KH, *et al.* The HIF-1 inhibitor YC-1 decreases reactive astrocyte formation in a rodent ischemia model. *Am J Transl Res*. 2015; 7: 751-60.
- [32] Chio CC, Lin JW, Cheng HA, Chiu WT, Wang YH, Wang JJ, *et al.* MicroRNA-210 targets antiapoptotic Bcl-2 expression and mediates hypoxia-induced apoptosis of neuroblastoma cells. *Arch Toxicol*. 2013; 87: 459-68.
- [33] Chou CW, Wang CC, Wu CP, Lin YJ, Lee YC, Cheng YW, *et al.* Tumor cycling hypoxia induces chemoresistance in glioblastoma multiforme by upregulating the expression and function of ABCB1. *Neuro Oncol*. 2012; 14: 1227-38.
- [34] Xiao J, Jin C, Liu Z, Guo S, Zhang X, Zhou X, *et al.* The design, synthesis, and biological evaluation of novel YC-1 derivatives as potent anti-hepatic fibrosis agents. *Org Biomol Chem*. 2015; 13: 7257-64.
- [35] Carroll CE, Liang Y, Benakanakere I, Besch-Williford C, Hyder SM. The anticancer agent YC-1 suppresses progesterin-stimulated VEGF in breast cancer cells and arrests breast tumor development. *Int J Oncol*. 2013; 42: 179-87.
- [36] Chen CJ, Hsu MH, Huang LJ, Yamori T, Chung JG, Lee FY, *et al.* Anticancer mechanisms of YC-1 in human lung cancer cell line, NCI-H226. *Biochem Pharmacol*. 2008; 75: 360-8.
- [37] Lee JC, Chou LC, Lien JC, Wu JC, Huang CH, Chung CH, *et al.* CLC604 preferentially inhibits the growth of HER2-overexpressing cancer cells and sensitizes these cells to the inhibitory effect of

- Taxol *in vitro* and *in vivo*. *Oncol Rep.* 2013; 30: 1762-72.
- [38] Lee SJ, Kim YJ, Lee CS, Bae J. Combined application of camptothecin and the guanylate cyclase activator YC-1: Impact on cell death and apoptosis-related proteins in ovarian carcinoma cell lines. *Chem Biol Interact.* 2009; 181: 185-92.
- [39] Flamigni F, Facchini A, Stanic I, Tantini B, Bonavita F, Stefanelli C. Control of survival of proliferating L1210 cells by soluble guanylate cyclase and p44/42 mitogen-activated protein kinase modulators. *Biochem Pharmacol* 2001; 62: 319-28.
- [40] Wang SX, Pei ZZ, Wu XH, Li JK, Yang YJ. Effect of YC-1 on HIF-1 alpha and VEGF expression in human hepatocarcinoma cell lines. *Zhonghua Gan Zang Bing Za Zhi.* 2009; 17: 308-9.
- [41] Li Y, Zhao X, Tang H, Zhong Z, Zhang L, Xu R, *et al.* Effects of YC-1 on hypoxia-inducible factor 1 alpha in hypoxic human bladder transitional carcinoma cell line T24 cells. *Urol Int.* 2012; 88: 95-101.
- [42] Zhao Q, Du J, Gu H, Teng X, Zhang Q, Qin H, *et al.* Effects of YC-1 on hypoxia-inducible factor 1-driven transcription activity, cell proliferative vitality, and apoptosis in hypoxic human pancreatic cancer cells. *Pancreas.* 2007; 34: 242-7.
- [43] Feng Y, Zhu H, Ling T, Hao B, Zhang G, Shi R. Effects of YC-1 targeting hypoxia-inducible factor 1 alpha in oesophageal squamous carcinoma cell line Eca109 cells. *Cell Biol Int.* 2011; 35: 491-7.
- [44] Lee CS, Kwak SW, Kim YJ, Lee SA, Park ES, Myung SC, *et al.* Guanylate cyclase activator YC-1 potentiates apoptotic effect of licochalcone A on human epithelial ovarian carcinoma cells *via* activation of death receptor and mitochondrial pathways. *Eur J Pharmacol.* 2012; 683: 54-62.
- [45] Liang D, Yang M, Guo B, Yang L, Cao J, Zhang X. HIF-1alpha induced by beta-elemene protects human osteosarcoma cells from undergoing apoptosis. *J Cancer Res Clin Oncol.* 2012; 138: 1865-77.
- [46] Chai ZT, Kong J, Zhu XD, Zhang YY, Lu L, Zhou JM, *et al.* MicroRNA-26a inhibits angiogenesis by down-regulating VEGFA through the PIK3C2alpha/Akt/HIF-1alpha pathway in hepatocellular carcinoma. *PLoS One.* 2013; 8: e77957.
- [47] Hong B, Lui VW, Hui EP, Lu Y, Leung HS, Wong EY, *et al.* Reverse phase protein array identifies novel anti-invasion mechanisms of YC-1. *Biochem Pharmacol.* 2010; 79: 842-52.
- [48] Tuttle TR, Takiar V, Kumar B, Kumar P, Ben-Jonathan N. Soluble guanylate cyclase stimulators increase sensitivity to cisplatin in head and neck squamous cell carcinoma cells. *Cancer Lett.* 2017; 389: 33-40.
- [49] Chou LC, Huang LJ, Yang JS, Lee FY, Teng CM, Kuo SC. Synthesis of furopyrazole analogs of 1-benzyl-3-(5-hydroxymethyl-2-furyl)indazole (YC-1) as novel anti-leukemia agents. *Bioorg Med Chem.* 2007; 15: 1732-40.
- [50] Wang SW, Pan SL, Guh JH, Chen HL, Huang DM, Chang YL, *et al.* YC-1 [3-(5'-Hydroxymethyl-2'-furyl)-1-benzyl Indazole] exhibits a novel antiproliferative effect and arrests the cell cycle in G0-G1 in human hepatocellular carcinoma cells. *J Pharmacol Exp Ther.* 2005; 312: 917-25.
- [51] Pan SL, Guh JH, Peng CY, Wang SW, Chang YL, Cheng FC, *et al.* YC-1 [3-(5'-hydroxymethyl-2'-furyl)-1-benzyl indazole] inhibits endothelial cell functions induced by angiogenic factors *in vitro* and angiogenesis *in vivo* models. *J Pharmacol Exp Ther.* 2005; 314: 35-42.
- [52] Kong J, Kong F, Gao J, Zhang Q, Dong S, Gu F, *et al.* YC-1 enhances the anti-tumor activity of sorafenib through inhibition of signal transducer and activator of transcription 3 (STAT3) in hepatocellular carcinoma. *Mol Cancer.* 2014; 13: 7.
- [53] Cheng Y, Li W, Liu Y, Cheng HC, Ma J, Qiu L. YC-1 exerts inhibitory effects on MDA-MB-468 breast cancer cells by targeting EGFR *in vitro* and *in vivo* under normoxic condition. *Chin J Cancer.* 2012; 31: 248-56.
- [54] Wu SY, Pan SL, Chen TH, Liao CH, Huang DY, Guh JH, *et al.* YC-1 induces apoptosis of human renal carcinoma A498 cells *in vitro* and *in vivo* through activation of the JNK pathway. *Br J Pharmacol.* 2008; 155: 505-13.
- [55] Chang LC, Lin HY, Tsai MT, Chou RH, Lee FY, Teng CM, *et al.* YC-1 inhibits proliferation of breast cancer cells by down-regulating EZH2 expression via activation of c-Cbl and ERK. *Br J Pharmacol.* 2014; 171: 4010-25.
- [56] Yeo EJ, Chun YS, Cho YS, Kim J, Lee JC, Kim MS, *et al.* YC-1: a potential anticancer drug targeting hypoxia-inducible factor 1. *J Natl Cancer Inst.* 2003; 95: 516-25.
- [57] Mullershausen F, Russwurm M, Friebe A, Koesling D. Inhibition of phosphodiesterase type 5 by the activator of nitric oxide-sensitive guanylyl cyclase BAY 41-2272. *Circulation.* 2004; 109: 1711-3.
- [58] Wang H, Kohr MJ, Traynham CJ, Ziolo MT. Phosphodiesterase 5 restricts NOS3/Soluble guanylate cyclase signaling to L-type Ca²⁺ current in cardiac myocytes. *J Mol Cell Cardiol.* 2009; 47: 304-14.
- [59] Chu PW, Beart PM, Jones NM. Preconditioning protects against oxidative injury involving hypoxia-inducible factor-1 and vascular endothelial growth factor in cultured astrocytes. *Eur J Pharmacol.* 2010; 633: 24-32.
- [60] Yeo EJ, Chun YS, Park JW. New anticancer strategies targeting HIF-1. *Biochem Pharmacol.* 2004; 68: 1061-9.
- [61] Ikezawa Y, Sakakibara-Konishi J, Mizugaki H, Oizumi S, Nishimura M. Inhibition of Notch and HIF enhances the antitumor effect of radiation in Notch expressing lung cancer. *Int J Clin Oncol.* 2017; 22: 59-69.
- [62] Wan J, Wu W, Huang Y, Ge W, Liu S. Incomplete radiofrequency ablation accelerates proliferation and angiogenesis of residual lung carcinomas *via* HSP70/HIF-1alpha. *Oncol Rep.* 2016; 36: 659-68.
- [63] Zhao T, Zhu Y, Morinibu A, Kobayashi M, Shinomiya K, Itasaka S, *et al.* HIF-1-mediated metabolic reprogramming reduces ROS levels and facilitates the metastatic colonization of cancers in lungs. *Sci Rep.* 2014; 4: 3793.
- [64] Nurwidya F, Takahashi F, Kobayashi I, Murakami A, Kato M, Minakata K, *et al.* Treatment with insulin-like growth factor 1 receptor inhibitor reverses hypoxia-induced epithelial-mesenchymal transition in non-small cell lung cancer. *Biochem Biophys Res Commun.* 2014; 455: 332-8.
- [65] Hsia TC, Liu WH, Qiu WW, Luo J, Yin MC. Maslinic acid induces mitochondrial apoptosis and suppresses HIF-1alpha expression in A549 lung cancer cells under normoxic and hypoxic conditions. *Molecules.* 2014; 19: 19892-906.
- [66] Kambayashi S, Igase M, Kobayashi K, Kimura A, Shimokawa Miyama T, Baba K, *et al.* Hypoxia inducible factor 1alpha expression and effects of its inhibitors in canine lymphoma. *J Vet Med Sci.* 2015; 77: 1405-12.

- [67] Chen WL, Wang CC, Lin YJ, Wu CP, Hsieh CH. Cycling hypoxia induces chemoresistance through the activation of reactive oxygen species-mediated B-cell lymphoma extra-long pathway in glioblastoma multiforme. *J Transl Med.* 2015; 13: 389.
- [68] Xue M, Li X, Li Z, Chen W. Urothelial carcinoma associated 1 is a hypoxia-inducible factor-1alpha-targeted long noncoding RNA that enhances hypoxic bladder cancer cell proliferation, migration, and invasion. *Tumour Biol.* 2014; 35: 6901-12.
- [69] Ma W, Shi X, Lu S, Wu L, Wang Y. Hypoxia-induced overexpression of DEC1 is regulated by HIF-1alpha in hepatocellular carcinoma. *Oncol Rep.* 2013; 30: 2957-62.
- [70] Aguilar H, Urruticoechea A, Halonen P, Kiyotani K, Mushiroda T, Barril X, *et al.* VAV3 mediates resistance to breast cancer endocrine therapy. *Breast Cancer Res.* 2014; 16: R53.
- [71] Lee CS, Kim YJ, Kim W, Myung SC. Guanylate cyclase activator YC-1 enhances TRAIL-induced apoptosis in human epithelial ovarian carcinoma cells *via* activation of apoptosis-related proteins. *Basic Clin Pharmacol Toxicol.* 2011; 109: 283-91.
- [72] Dai Y, Bae K, Siemann DW. Impact of hypoxia on the metastatic potential of human prostate cancer cells. *Int J Radiat Oncol Biol Phys.* 2011; 81: 521-8.
- [73] Wang L, Zhou W, Gou S, Wang T, Liu T, Wang C. Insulin promotes proliferative vitality and invasive capability of pancreatic cancer cells via hypoxia-inducible factor 1alpha pathway. *J Hua-zhong Univ Sci Technolog Med Sci.* 2010; 30: 349-53.
- [74] Cho IR, Koh SS, Min HJ, Park EH, Ratakorn S, Jhun BH, *et al.* Down-regulation of HIF-1alpha by oncolytic reovirus infection independently of VHL and p53. *Cancer Gene Ther.* 2010; 17: 365-72.
- [75] Aubert S, Fauquette V, Hemon B, Lepoivre R, Briez N, Bernard D, *et al.* MUC1, a new hypoxia inducible factor target gene, is an actor in clear renal cell carcinoma tumor progression. *Cancer Res.* 2009; 69: 5707-15.
- [76] Deguchi A, Xing SW, Shureiqi I, Yang P, Newman RA, Lippman SM, *et al.* Activation of protein kinase G up-regulates expression of 15-lipoxygenase-1 in human colon cancer cells. *Cancer Res.* 2005; 65: 8442-7.
- [77] Liu L, Li H, Underwood T, Lloyd M, David M, Sperl G, *et al.* Cyclic GMP-dependent protein kinase activation and induction by exisulind and CP461 in colon tumor cells. *J Pharmacol Exp Ther.* 2001; 299: 583-92.
- [78] Wang F, Chen BA, Cheng J, Xu WL, Wang XM, Ding JH, *et al.* Effects of hypoxia-inducible factor inhibitor on expression of HIF-1alpha and VEGF and induction of apoptosis in leukemic cell lines. *Zhongguo Shi Yan Xue Ye Xue Za Zhi.* 2010; 18: 74-8.
- [79] Hsu HK, Juan SH, Ho PY, Liang YC, Lin CH, Teng CM, *et al.* YC-1 inhibits proliferation of human vascular endothelial cells through a cyclic GMP-independent pathway. *Biochem Pharmacol.* 2003; 66: 263-71.
- [80] Chiang WC, Teng CM, Lin SL, Chen YM, Tsai TJ, Hsieh BS. YC-1-inhibited proliferation of rat mesangial cells through suppression of cyclin D1-independent of cGMP pathway and partially reversed by p38 MAPK inhibitor. *Eur J Pharmacol.* 2005; 517: 1-10.
- [81] Yeo EJ, Ryu JH, Chun YS, Cho YS, Jang IJ, Cho H, *et al.* YC-1 induces S cell cycle arrest and apoptosis by activating checkpoint kinases. *Cancer Res.* 2006; 66: 6345-52.
- [82] Hung CC, Liou HH. YC-1, a novel potential anticancer agent, inhibit multidrug-resistant protein via cGMP-dependent pathway. *Invest New Drugs.* 2011; 29: 1337-46.
- [83] Zhou Q, Liu H, Sun Q, Zhang L, Lin H, Yuan G, *et al.* Adenosine monophosphate-activated protein kinase/mammalian target of rapamycin-dependent autophagy protects human dental pulp cells against hypoxia. *J Endod.* 2013; 39: 768-73.
- [84] Tung JN, Cheng YW, Hsu CH, Liu TZ, Hsieh PY, Ting LL, *et al.* Normoxically overexpressed hypoxia inducible factor 1-alpha is involved in arsenic trioxide resistance acquisition in hepatocellular carcinoma. *Ann Surg Oncol.* 2011; 18: 1492-500.
- [85] Hsieh MT, Chen HP, Lu CC, Chiang JH, Wu TS, Kuo DH, *et al.* The novel pterostilbene derivative ANK-199 induces autophagic cell death through regulating PI3 kinase class III/beclin 1/Atg-related proteins in cisplatinresistant CAR human oral cancer cells. *Int J Oncol.* 2014; 45: 782-94.
- [86] Chang PY, Peng SF, Lee CY, Lu CC, Tsai SC, Shieh TM, *et al.* Curcumin-loaded nanoparticles induce apoptotic cell death through regulation of the function of MDR1 and reactive oxygen species in cisplatin-resistant CAR human oral cancer cells. *Int J Oncol.* 2013; 43: 1141-50.
- [87] Yang JS, Chen GW, Hsia TC, Ho HC, Ho CC, Lin MW, *et al.* Di-allyl disulfide induces apoptosis in human colon cancer cell line (COLO 205) through the induction of reactive oxygen species, endoplasmic reticulum stress, caspases cascade and mitochondrial-dependent pathways. *Food Chem Toxicol.* 2009; 47: 171-9.
- [88] Lai KC, Huang AC, Hsu SC, Kuo CL, Yang JS, Wu SH, *et al.* Benzyl isothiocyanate (BITC) inhibits migration and invasion of human colon cancer HT29 cells by inhibiting matrix metalloproteinase-2/-9 and urokinase plasminogen (uPA) through PKC and MAPK signaling pathway. *J Agric Food Chem.* 2010; 58: 2935-42.
- [89] Huang WW, Chiu YJ, Fan MJ, Lu HF, Yeh HF, Li KH, *et al.* Kaempferol induced apoptosis *via* endoplasmic reticulum stress and mitochondria-dependent pathway in human osteosarcoma U-2 OS cells. *Mol Nutr Food Res.* 2010; 54: 1585-95.
- [90] Chang WM, Lin YF, Su CY, Peng HY, Chang YC, Hsiao JR, *et al.* Parathyroid Hormone-Like Hormone is a Poor Prognosis Marker of Head and Neck Cancer and Promotes Cell Growth *via* RUNX2 Regulation. *Sci Rep.* 2017; 7: 41131.
- [91] Chiu YJ, Hour MJ, Lu CC, Chung JG, Kuo SC, Huang WW, *et al.* Novel quinazoline HMJ-30 induces U-2 OS human osteogenic sarcoma cell apoptosis through induction of oxidative stress and up-regulation of ATM/p53 signaling pathway. *J Orthop Res.* 2011; 29: 1448-56.
- [92] Yang JS, Hour MJ, Kuo SC, Huang LJ, Lee MR. Selective induction of G2/M arrest and apoptosis in HL-60 by a potent anticancer agent, HMJ-38. *Anticancer Res.* 2004; 24: 1769-78.
- [93] Lin CF, Yang JS, Lin C, Tsai FJ, Lu CC, Lee MR. CCY-1a-E2 induces G2/M phase arrest and apoptotic cell death in HL-60 leukemia cells through cyclin-dependent kinase 1 signaling and the mitochondria-dependent caspase pathway. *Oncol Rep.* 2016; 36: 1633-9.
- [94] Lai KC, Lu CC, Tang YJ, Chiang JH, Kuo DH, Chen FA, *et al.* Allyl isothiocyanate inhibits cell metastasis through suppression of the MAPK pathways in epidermal growth factorstimulated HT29 human colorectal adenocarcinoma cells. *Oncol Rep.* 2014; 31: 189-96.
- [95] Huang WW, Tsai SC, Peng SF, Lin MW, Chiang JH, Chiu YJ, *et al.*

- Kaempferol induces autophagy through AMPK and AKT signaling molecules and causes G2/M arrest via downregulation of CDK1/cyclin B in SK-HEP-1 human hepatic cancer cells. *Int J Oncol.* 2013; 42: 2069-77.
- [96] Chen YF, Yang JS, Chang WS, Tsai SC, Peng SF, Zhou YR. Houttuynia cordata Thunb extract modulates G₀/G₁ arrest and Fas/CD95-mediated death receptor apoptotic cell death in human lung cancer A549 cells. *J Biomed Sci.* 2013; 20: 18.
- [97] Liu CY, Yang JS, Huang SM, Chiang JH, Chen MH, Huang LJ, *et al.* Smh-3 induces G(2)/M arrest and apoptosis through calcium-mediated endoplasmic reticulum stress and mitochondrial signaling in human hepatocellular carcinoma Hep3B cells. *Oncol Rep.* 2013; 29: 751-62.
- [98] Huang SH, Wu LW, Huang AC, Yu CC, Lien JC, Huang YP, *et al.* Benzyl isothiocyanate (BITC) induces G2/M phase arrest and apoptosis in human melanoma A375.S2 cells through reactive oxygen species (ROS) and both mitochondria-dependent and death receptor-mediated multiple signaling pathways. *J Agric Food Chem.* 2012; 60: 665-75.
- [99] Ma CY, Ji WT, Chueh FS, Yang JS, Chen PY, Yu CC, *et al.* Butein inhibits the migration and invasion of SK-HEP-1 human hepatocarcinoma cells through suppressing the ERK, JNK, p38, and uPA signaling multiple pathways. *J Agric Food Chem.* 2011; 59: 9032-8.
- [100] Chiang JH, Yang JS, Lu CC, Hour MJ, Chang SJ, Lee TH, *et al.* Newly synthesized quinazolinone HMJ-38 suppresses angiogenetic responses and triggers human umbilical vein endothelial cell apoptosis through p53-modulated Fas/death receptor signaling. *Toxicol Appl Pharmacol.* 2013; 269: 150-62.
- [101] Lu CC, Yang JS, Chiang JH, Hour MJ, Lin KL, Lee TH, *et al.* Cell death caused by quinazolinone HMJ-38 challenge in oral carcinoma CAL 27 cells: dissections of endoplasmic reticulum stress, mitochondrial dysfunction and tumor xenografts. *Biochim Biophys Acta.* 2014; 1840: 2310-20.
- [102] Lin C, Tsai SC, Tseng MT, Peng SF, Kuo SC, Lin MW, *et al.* AKT serine/threonine protein kinase modulates baicalin-triggered autophagy in human bladder cancer T24 cells. *Int J Oncol.* 2013; 42: 993-1000.
- [103] Tsai SC, Yang JS, Peng SF, Lu CC, Chiang JH, Chung JG, *et al.* Bufalin increases sensitivity to AKT/mTOR-induced autophagic cell death in SK-HEP-1 human hepatocellular carcinoma cells. *Int J Oncol.* 2012; 41: 1431-42.
- [104] Lu CC, Yang JS, Chiang JH, Hour MJ, Lin KL, Lin JJ, *et al.* Novel quinazolinone MJ-29 triggers endoplasmic reticulum stress and intrinsic apoptosis in murine leukemia WEHI-3 cells and inhibits leukemic mice. *PLoS One.* 2012; 7: e36831.
- [105] Peng SF, Lee CY, Hour MJ, Tsai SC, Kuo DH, Chen FA, *et al.* Curcumin-loaded nanoparticles enhance apoptotic cell death of U2OS human osteosarcoma cells through the Akt-Bad signaling pathway. *Int J Oncol.* 2014; 44: 238-46.
- [106] Tsai YF, Huang CW, Chiang JH, Tsai FJ, Hsu YM, Lu CC, *et al.* Gadolinium chloride elicits apoptosis in human osteosarcoma U-2 OS cells through extrinsic signaling, intrinsic pathway and endoplasmic reticulum stress. *Oncol Rep.* 2016; 36: 3421-26.
- [107] Mason JM, Wei X, Fletcher GC, Kiarash R, Brox R, Hodgson R, *et al.* Functional characterization of CFI-402257, a potent and selective Mps1/TTK kinase inhibitor, for the treatment of cancer. *Proc Natl Acad Sci U S A.* 2017; 114: 3127-32.
- [108] Hour MJ, Lee KH, Chen TL, Lee KT, Zhao Y, Lee HZ. Molecular modelling, synthesis, cytotoxicity and anti-tumour mechanisms of 2-aryl-6-substituted quinazolinones as dual-targeted anti-cancer agents. *Br J Pharmacol.* 2013; 169: 1574-86.
- [109] Sarkar J, Singh N, Meena S, Sinha S. Staurosporine induces apoptosis in human papillomavirus positive oral cancer cells at G2/M phase by disrupting mitochondrial membrane potential and modulation of cell cytoskeleton. *Oral Oncol.* 2009; 45: 974-9.
- [110] Carlson RO. New tubulin targeting agents currently in clinical development. *Expert Opin Investig Drugs.* 2008; 17: 707-22.
- [111] Tsui L, Fong TH, Wang IJ. The effect of 3-(5'-hydroxymethyl-2'-furyl)-1-benzylindazole (YC-1) on cell viability under hypoxia. *Mol Vis.* 2013; 19: 2260-73.
- [112] Huang YT, Pan SL, Guh JH, Chang YL, Lee FY, Kuo SC, *et al.* YC-1 suppresses constitutive nuclear factor-kappaB activation and induces apoptosis in human prostate cancer cells. *Mol Cancer Ther.* 2005; 4: 1628-35.
- [113] Zhang Q, Bian H, Guo L, Zhu H. Pharmacologic preconditioning with berberine attenuating ischemia-induced apoptosis and promoting autophagy in neuron. *Am J Transl Res.* 2016; 8: 1197-207.
- [114] Yeh CH, Hsu SP, Yang CC, Chien CT, Wang NP. Hypoxic preconditioning reinforces HIF-alpha-dependent HSP70 signaling to reduce ischemic renal failure-induced renal tubular apoptosis and autophagy. *Life Sci.* 2010; 86: 115-23.
- [115] Wu J, Ke X, Wang W, Zhang H, Ma N, Fu W, *et al.* Aloe-emodin suppresses hypoxia-induced retinal angiogenesis via inhibition of HIF-1alpha/VEGF pathway. *Int J Biol Sci.* 2016; 12: 1363-71.
- [116] Chang LH, Pan SL, Lai CY, Tsai AC, Teng CM. Activated PAR-2 regulates pancreatic cancer progression through ILK/HIF-alpha-induced TGF-alpha expression and MEK/VEGF-A-mediated angiogenesis. *Am J Pathol.* 2013; 183: 566-75.
- [117] Liu YN, Pan SL, Peng CY, Guh JH, Huang DM, Chang YL, *et al.* YC-1 [3-(5'-hydroxymethyl-2'-furyl)-1-benzyl indazole] inhibits neointima formation in balloon-injured rat carotid through suppression of expressions and activities of matrix metalloproteinases 2 and 9. *J Pharmacol Exp Ther.* 2006; 316: 35-41.
- [118] Shin DH, Kim JH, Jung YJ, Kim KE, Jeong JM, Chun YS, *et al.* Preclinical evaluation of YC-1, a HIF inhibitor, for the prevention of tumor spreading. *Cancer Lett.* 2007; 255: 107-16.
- [119] Kim HL, Yeo EJ, Chun YS, Park JW. A domain responsible for HIF-1alpha degradation by YC-1, a novel anticancer agent. *Int J Oncol.* 2006; 29: 255-60.
- [120] Lau CK, Yang ZF, Lam SP, Lam CT, Ngai P, Tam KH, *et al.* Inhibition of Stat3 activity by YC-1 enhances chemo-sensitivity in hepatocellular carcinoma. *Cancer Biol Ther.* 2007; 6: 1900-7.
- [121] Birkinshaw RW, Czabotar PE. The BCL-2 family of proteins and mitochondrial outer membrane permeabilisation. *Semin Cell Dev Biol.* 2017.
- [122] Shakeri R, Kheirollahi A, Davoodi J. Apaf-1: Regulation and function in cell death. *Biochimie.* 2017; 135: 111-25.
- [123] Li P, Zhou L, Zhao T, Liu X, Zhang P, Liu Y, *et al.* Caspase-9: structure, mechanisms and clinical application. *Oncotarget.* 2017; 8: 23996-4008.
- [124] Maes ME, Schlamp CL, Nickells RW. BAX to basics: How the BCL2 gene family controls the death of retinal ganglion cells. *Prog Retin Eye Res.* 2017; 57: 1-25.
- [125] Ho TF, Chang CC. A promising "TRAIL" of tanshinones for can-

- cer therapy. *Biomedicine (Taipei)*. 2015; 5: 23.
- [126] Harma V, Schukov HP, Happonen A, Ahonen I, Virtanen J, Siitari H, *et al.* Quantification of dynamic morphological drug responses in 3D organotypic cell cultures by automated image analysis. *PLoS One*. 2014; 9: e96426.
- [127] Single A, Beetham H, Telford BJ, Guilford P, Chen A. A Comparison of Real-Time and Endpoint Cell Viability Assays for Improved Synthetic Lethal Drug Validation. *J Biomol Screen*. 2015; 20: 1286-93.
- [128] Bain JM, Louw J, Lewis LE, Okai B, Walls CA, Ballou ER, *et al.* *Candida albicans* hypha formation and mannan masking of beta-glucan inhibit macrophage phagosome maturation. *MBio*. 2014; 5: e01874.